Article
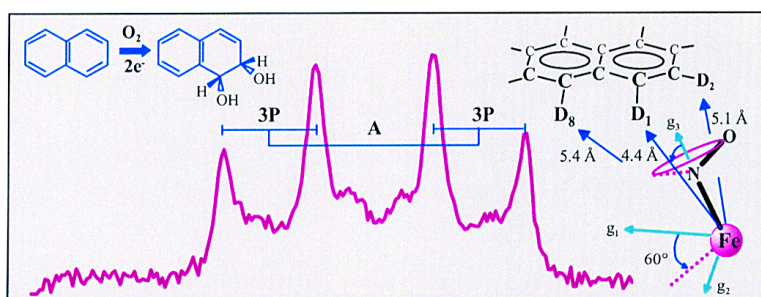
Substrate Binding to NO–Ferro–Naphthalene 1,2-Dioxygenase Studied by High-Resolution Q-Band Pulsed H-ENDOR Spectroscopy

Tran Chin Yang, Matt D. Wolfe, Matthew B. Neibergall, Yasmina Mekmouche, John D. Lipscomb, and Brian M. Hoffman

More About This Article

Additional resources and features associated with this article are available within the HTML version:

- Supporting Information
- Links to the 7 articles that cite this article, as of the time of this article download
- Access to high resolution figures
- Links to articles and content related to this article
- Copyright permission to reproduce figures and/or text from this article

View the Full Text HTML

Substrate Binding to NO−Ferro−Naphthalene 1,2-Dioxygenase Studied by High-Resolution Q-Band Pulsed ²H-ENDOR Spectroscopy

Tran Chin Yang,[†] Matt D. Wolfe,[‡,§] Matthew B. Neibergall,[‡] Yasmina Mekmouche,[‡] John D. Lipscomb,*[,‡] and Brian M. Hoffman*[,†]

Contribution from the Department of Chemistry, Northwestern University, Evanston, Illinois 60208-3113, and Department of Biochemistry, Molecular Biology, and Biophysics and the Center for Metals in Biocatalysis, University of Minnesota, 321 Church Street SE, Minneapolis, Minnesota 55455

Received December 5, 2002; E-mail: bmh@northwestern.edu

Abstract: The active site of naphthalene 1,2-dioxygenase (NDO) contains a Rieske Fe−S cluster and a mononuclear non-heme iron, which are contributed by different α-subunits in the $(\alpha\beta)_3$ structure. The enzyme catalyzes *cis*-dihydroxylation of aromatic substrates, in addition to numerous other adventitious oxidation reactions. High-resolution Mims ²H-ENDOR (electron nuclear double resonance) spectra have been recorded for the NO−ferrous center of NDO bound with the substrates d_8-naphthalene, d_2-naphthalene, d_8-toluene, d_3-toluene, and d_6-benzene; samples were prepared in a D_2O buffer to test for solvent-derived ligands; spectra were collected for enzymes with the Rieske diiron center in both its oxidized and reduced states. A sharp quartet ENDOR pattern from a nearby deuteron of the substrate in a major binding geometry (denoted as A) was detected for all perdeuterated substrates. Examination of the sample prepared with 1,4-di-deutero-naphthalene shows that the signal arises from D1. Analysis of two-dimensional (2-D) orientation-selective ENDOR patterns collected for this sample defined the location of the D1 deuteron, with respect to the *g*-frame of the iron center and the orientation of the C−D1 bond. Consideration of the orientations of naphthalene that are permitted within the constraints of these results, as supported by a novel approach to simulations of orientation-selective, 2-D ENDOR patterns for the perdeuterated naphthalene sample, which summed contributions from D1/D2/D8, disclose the geometry of the naphthalene and the Fe−NO fragment. The two deuterons of the reactive carbons, D1 and D2, are closest to the Fe atom ($r_{Fe-D1} \approx 4.3$ Å, $r_{Fe-D2} \approx 5.0$ Å), whereas D8 is farther away ($r_{Fe-D8} \approx 5.3$ Å). Perhaps more instructive, D1−N and D2−N distances to the O_2 surrogate, NO, are ∼2.4 and ∼3.3 Å, respectively, whereas the D8−N distance is ∼3.7 Å. The data show that benzene and the aromatic ring of toluene also sit within the substrate-binding pocket adjacent to the mononuclear Fe atom. These rings occupy a position similar to that of the "proximal" ring of naphthalene, with the closest ring deuteron being located at a distance of ∼4.3−4.4 Å from the Fe atom and with the Fe−D vector being slightly off the Fe−N(O) direction. In particular, comparison of the data for d_8-toluene and methyl-d_3-toluene shows that the methyl group of toluene points away from the Fe atom, despite observations that the oxidation of toluene occurs at the methyl group during catalysis. The Rieske cluster is reduced during both steady-state and single-turnover catalysis; therefore, the effect of its oxidation state on the geometry of substrate binding was examined. The spectra from the NDO−naphthalene complex also revealed a second binding conformation (denoted as B), in which the substrate is located ∼0.5 Å farther from the Fe atom. The relative populations of A- and B-sites are allosterically changed when the Rieske cluster is reduced. ENDOR of exchangeable protons shows that the water/hydroxide of Fe−NDO is retained upon binding NO.

Introduction

The naphthalene 1,2-dioxygenase (NDO) system from *Pseudomonas* sp. NCIB 9816-4 catalyzes the *cis*-dihydroxylation of naphthalene to yield *cis*-(1R,2S)-dihydroxy-1,2-dihydronaph-thalene as a key step in the biological assimilation of carbon from naphthalene.[1,2] The NDO system consists of a 36 kDa reductase (NDR), a 14 kDa ferredoxin (NDF), and a 210 kDa $(\alpha\beta)_3$ oxygenase (NDO) component that, together, function to shuttle electrons from the reduced pyridine nucleotide to the active site of NDO where O_2 activation and substrate hydroxylation occur.[3,4]

* Corresponding author.
† Northwestern University.
‡ University of Minnesota.
§ Current address: Laboratory of Biochemistry, National Heart, Lung and Blood Institute, National Institutes of Health, 2122 MSC-8012, 50 South Dr., Bethesda, MD 20892.

(1) Jeffrey, A. M.; Yeh, H. J. C.; Jerina, D. M.; Patel, T. R.; Davey, J. F.; Gibson, D. T. *Biochemistry* **1975**, *14*, 575−584.
(2) Gibson, D. T.; Parales, R. E. *Curr. Opin. Biotechnol.* **2000**, *11*, 236−243.
(3) Ensley, B. D.; Gibson, D. T. *J. Bacteriol.* **1983**, *155*, 505−511.
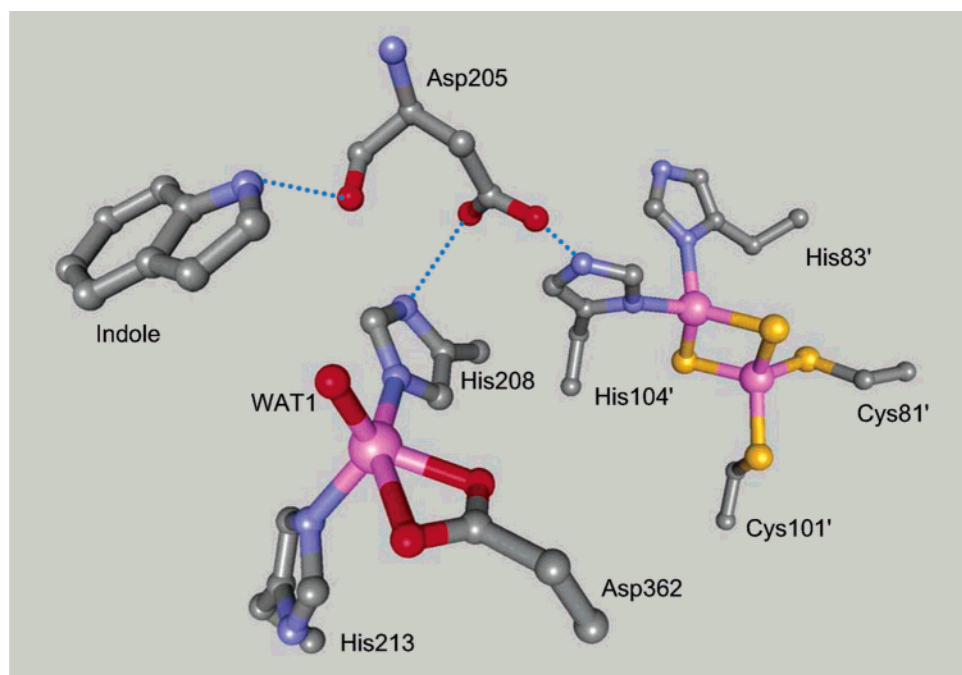
Figure 1. Structure of NDO[R] with bound indole, see ref 5.[4]

The crystal structure of NDO shows each α-subunit to contain a Rieske-type center [2Fe2S] and a mononuclear iron center, separated by ~44 Å.[4] However, the active pair is thought to be a neighboring Rieske cluster and mononuclear iron that are separated by ~12 Å, with naphthalene and O_2 binding at the catalytic mononuclear iron site. Furthermore, the initial structural studies of NDO revealed that the alternative substrate indole binds within 5 Å of the mononuclear iron in a location consistent with the observed hydroxylation of the pyrrole ring (Figure 1).[5] Interestingly, it was discovered that the Rieske cluster is readily reduced upon exposure to the X-ray beam during structural data collection.[6] Thus, all the available NDO structures represent the conformation in which both the Rieske cluster and the mononuclear iron are reduced (denoted as ferro–NDO[R]). More recently, our spectroscopic and kinetic studies established that NDO alone can catalyze *cis*-dihydroxylation of naphthalene in a single-turnover reaction if both the Rieske and mononuclear iron centers are reduced at the start of the reaction.[7] It was further shown that oxygen binding at the mononuclear center is gated by both substrate binding *and* Rieske cluster reduction, implying that there is some structural reorganization that occurs during these processes. This type of regulation would prevent activation of molecular oxygen before the substrate is present in the active site and, thus, avoid uncoupled turnover and uncontrolled production of reactive oxygen species. Finally, these studies showed that NO acts as an oxygen surrogate that can bind to the mononuclear center, regardless of the oxidation state of the Rieske cluster.

Although it is clear that a fully reduced enzyme is required for turnover in the reductive oxygen activation pathway, it has been shown that the substrate can bind to the enzyme in which only the mononuclear iron is reduced (denoted as ferro–NDO). Substrate binding causes changes in the electron paramagnetic resonance (EPR) spectrum of the nitrosyl–ferrous complex of the mononuclear iron, which exhibits resonances near $g = 4$ and 2, which are characteristic of an $S = \frac{3}{2}$ species.[7] In the related phthalate dioxygenase, NMR relaxation studies of a Co-(II)-substituted enzyme indicated that the substrate lies ~5 Å from the Co atom, with the Rieske cluster in the oxidized state.[8] It remains unclear whether, during the NDO catalytic cycle, the enzyme first binds the substrate or first accepts an electron at the Rieske cluster. However, it seems likely, on the basis of our recent studies of benzoate dioxygenase, that the mononuclear center must be reduced to release product, and thus, it is likely to be in the ferrous oxidation state as the substrate binds in the next cycle.[9]

In addition to *cis*-dihydroxylation, the NDO system catalyzes most other types of O_2-dependent reactions.[10] Some substrates, such as toluene, primarily undergo side chain hydroxylation in a monooxygenase reaction rather than *cis*-dihydroxylation.[11] Other single-ring substrates, such as benzene, primarily cause uncoupling of the reaction to yield hydrogen peroxide rather than substrate oxidation.[12] Inspection of the crystal structure of the indole complex of the fully reduced enzyme has led to speculation that the single-ring compounds bind in a site designed for the distal ring of two-ring substrates, and, thus, they are not optimally positioned for *cis*-diol-forming oxygenase chemistry to occur.[5] Similar positioning of toluene might bring the side chain into the vicinity of the activated oxygen species at the mononuclear iron and lead to its oxidation.

(4) Kauppi, B.; Lee, K.; Carredano, E.; Parales, R. E.; Gibson, D. T.; Eklund, H.; Ramaswamy, S. *Structure (London)* **1998**, *6*, 571−586.
(5) Carredano, E.; Karlsson, A.; Kauppi, B.; Choudhury, D.; Parales, R. E.; Parales, J. V.; Lee, K.; Gibson, D. T.; Eklund, H.; Ramaswamy, S. *J. Mol. Biol.* **2000**, *296*, 701−712.
(6) Karlsson, A.; Parales, J. V.; Parales, R. E.; Gibson, D. T.; Eklund, H.; Ramaswamy, S. *J. Inorg. Biochem.* **2000**, *78*, 83−87.
(7) Wolfe, M. D.; Parales, J. V.; Gibson, D. T.; Lipscomb, J. D. *J. Biol. Chem.* **2001**, *276*, 1945−1953.

(8) Tierney, D. L.; Gassner, G. T.; Luchinat, C.; Bertini, I.; Ballou, D. P.; Penner-Hahn, J. E. *Biochemistry* **1999**, *38*, 11051−11061.
(9) Wolfe, M. D.; Altier, D. J.; Stubna, A.; Popescu, C. V.; Codrina, V.; Münck, E.; Lipscomb, J. *Biochemistry* **2002**, *41*, 9611−9626.
(10) Resnick, S. M.; Lee, K.; Gibson, D. T. *J. Ind. Microbiol. Biotechnol.* **1996**, *17*, 438−457.
(11) Lee, K.; Gibson, D. T. *Appl. Environ. Microbiol.* **1996**, *62*, 3101−3106.
(12) Lee, K. *J. Bacteriol.* **1999**, *181*, 2719−2725.

Here, we report the use of Q-band pulsed deuteron electron nuclear double resonance (ENDOR) to study the complexes of NO−ferro−NDO with deuterated naphthalenes, toluenes, and benzene, each with the Rieske cluster in both the oxidized and reduced states. These studies employ a novel analysis procedure to obtain precise information about the position of naphthalene bound in the active site, as well as similar information about the other substrates. They provide the first information about substrate binding while an oxygen surrogate is bound to the Fe ion, as well as the first information about the substrate binding to the iron-containing enzyme with an oxidized Rieske cluster. Comparison with an X-ray diffraction study of the ferro−NDO[R]−naphthalene adduct, which was reported while the current paper was under review,[13] confirms that NO is a good surrogate for O_2 in this system, whereas the X-ray structures of complexes formed *in crystals* are seen to be in accord with structural information derived from enzymes frozen after making complexes *in solution*. The present study further discloses that the methyl group of toluene points away from the Fe atom, despite observations that the oxidation of toluene occurs at the methyl group during catalysis. Perhaps most intriguing, as described in a preliminary report,[14] deuteron ENDOR measurements show that reduction of the Rieske cluster allosterically modulates the geometry of the substrate binding, providing the first insight into the link between cluster reduction and regulation of the oxygen activation process.

Materials and Methods

Chemicals. Water was deionized and then purified using a Millipore ultrafiltration system. ($^2H_8$)-naphthalene, (^2H_3C)-toluene, and ($^2H_6$)-benzene were purchased from Isotech. ($^2H_8$)-toluene was obtained from Cambridge. All other isotopes were purchased from Sigma-Aldrich. NO gas (Matheson) was further purified by bubbling it through 6 N NaOH. All other chemicals (Sigma-Aldrich) were analytical grade and used without further purification.

Protein and Sample Preparation. NDO used in this study was purified from *Pseudomonas* sp. NCIB 9816-4, as described previously.[7] All samples used for spectroscopic measurements were prepared in 100 mM MES pH 6.8, 10% glycerol. When required, buffers were prepared in ^2H_2O, glycerol ($H_5C_3O_3{}^2H_3$) and adjusted to a pH of 6.4 (p^2H 6.8), using ^2HCl or NaO^2H. NDO was first made anaerobic by flushing the surface of the solution with argon for 20 min. The enzyme was then diluted fourfold with a buffer or buffer saturated with naphthalene (250 μM), toluene (6 mM), or benzene (23 mM). The protein solution was then concentrated using Centricon 100 (Amicon) and the dilution/concentration procedure was repeated two more times, with the final protein concentration for all samples being ~2 mM NDO active sites ($\alpha\beta$). The protein was transferred to a small septum-sealed reaction vial and flushed with argon for 2 min. Nitrosyl complexes were made by flushing the surface of the stirred sample with NO for 1 min, transferring the protein to an anaerobic quartz ENDOR tube, and quickly freezing the sample in liquid nitrogen. The NO−ferro−NDO samples thus prepared contain an oxidized Rieske center. To prepare ferro−NDO enzyme, in which the Rieske center is in the reduced state (denoted as NO−ferro−NDO[R]), the NO−ferro−NDO samples were thawed under an anaerobic atmosphere and 5 μL of an anaerobic solution of 100 mM sodium dithionite and 200 μM methyl viologen in 100 mM MES pH 6.8, 10% glycerol were added to establish a fivefold excess of reducing equivalents over the concentration of NDO subunits

present. After a 10 min incubation, the sample was frozen by slow emersion in liquid nitrogen and the EPR spectrum was recorded to verify that the characteristic signals of the reduced Rieske cluster and mononuclear iron−NO complex were both present. The EPR signal of reduced methyl viologen was also observed, showing that the enzyme was fully reduced.

EPR and ENDOR Spectroscopy. X-band EPR spectra were recorded on Bruker model E-500 instrument equipped with an Oxford model ESR-910 liquid helium cryostat. ENDOR spectra were recorded at 2 K on a pulsed Q-band spectrometer that has been described previously.[15,16] For small hyperfine couplings, the Mims ENDOR pulse sequence ($\pi/2-\tau-\pi/2-T-\pi/2-\tau-$echo) was applied.[17] The Mims sequence has a response of the form $R = 1 - \cos(2\pi A\tau)$ and, thus, has "blind spots" at $A\tau = n$. The maximum hyperfine coupling that can be detected such that the entire pattern falls within the $n = 1$ blind spot (A_{max}) is limited by the applicable shortest useful τ (the dead time, τ_d); the spectrometer is not optimized for a short dead time, and, as a result, $A_{max} \approx 1/(2\tau_d) \approx 2$ MHz in the present experiments. For bigger hyperfine couplings, the refocused Mims sequence ($\pi/2-\tau_1-\pi/2-T-\pi/2-\tau_2-\pi-[\tau_1+\tau_2]-$echo) was used.[18] In both pulse sequences, T represents the rf pulse length; T values of 20 and 60 μs were employed in the present experiments. It is possible to do quantitative studies with pulsed ENDOR because, in general, the absolute ENDOR intensity in a pulsed ENDOR spectrum, which is defined as the ratio of the ENDOR effect (change in spin−echo intensity with resonant RF excitation) to the intensity of the unperturbed spin−echo, is a good measure of the number of interacting nuclei.

The ENDOR pattern for a nucleus with spin $I = {}^1/_2$ exhibits paired features that, to first order, are given by[19]

$$\nu(\pm, m) = |\nu_n \pm \frac{A}{2} + (2m - 1)\frac{3P}{2}| \tag{1}$$

where $m = I, I - 1, \geq 0$, ν_n is the nuclear Larmor frequency, and A and $3P$ are the orientation-dependent hyperfine and quadrupole coupling constants. For the Q-band $^2H(I = 1)$ ENDOR spectra we report, $\nu_D \gg A$ and $3P$, and the equation gives a four-line pattern comprised of two branches, denoted as the ($\pm$) branches, which are separated by A and centered at ν_D, with each branch split into two peaks by the quadrupole splitting, $3P$. The EPR signal of NO−ferrous−NDO arises from transitions within the $m_s = \pm$ doublet of an $S = {}^3/_2$ electron-spin system.[20] In this case, the components of the *observed*, or *effective*, hyperfine tensor, denoted here as A', are scaled relative to the *intrinsic* interaction tensor of the $S = {}^3/_2$ state through scaling by the g-values that describe the EPR signal within the doublet;[21,22] for example, if the g and A tensors are coaxial (which was *not* assumed to be the case during analysis of the ENDOR spectra), one would have an *observed* tensor with components $A' = [A_1', A_2', A_3'] = [(g_1/g_e)A_1, (g_2/g_e)A_2, (g_3/g_e)A_3]$, where the A_i terms are the *intrinsic* tensor components.[22] In the body of this paper, we commonly suppress the prime symbol and talk of the *hyperfine* interaction (when we mean the *observed* interaction) and *the intrinsic* interaction when appropriate. Simulations of two-dimensional (2-D) patterns of ENDOR spectra collected at multiple fields across an EPR envelope are performed as described.[23] The simulations of a dipolar hyperfine interaction between a nucleus and

(13) Karlsson, A.; Parales, J. V.; Parales, R. E.; Gibson, D. T.; Eklund, H.; Ramaswamy, S. *Science (Washington, D.C.)* **2003**, *299*, 1039−1042.
(14) Yang, T.-C.; Wolfe, M. D.; Neibergall, M. B.; Mekmouche, Y.; Lipscomb, J.; Hoffman, B. *J. Am. Chem. Soc.* **2003**, *125*, 2034−2035.

(15) Fan, C.; Doan, P. E.; Davoust, C. E.; Hoffman, B. M. *J. Magn. Res.* **1992**, *98*, 62−72.
(16) Davoust, C. E.; Doan, P. E.; Hoffman, B. M. *J. Magn. Reson.* **1996**, *119*, 38−44.
(17) Mims, W. B. *Proc. R. Soc. London* **1965**, *283*, 452−457.
(18) Doan, P. E.; Hoffman, B. M. *Chem. Phys. Lett.* **1997**, *269*, 208−214.
(19) DeRose, V. J.; Hoffman, B. M. In *Biochemical Spectroscopy*; Sauer, K., Ed.; Methods in Enzymology 246; Academic Press: New York, 1995; pp 554−589.
(20) Brown, C. A.; Pavlosky, M. A.; Westre, T. E.; Zhang, Y.; Hedman, B.; Hodgson, K. O.; Solomon, E. I. *J. Am. Chem. Soc.* **1995**, *117*, 715−732.
(21) Hutchison, C. A., Jr.; McKay, D. B. *J. Chem. Phys.* **1977**, *66*, 3311−3330.
(22) Hoffman, B. M.; Gurbiel, R. J.; Werst, M. M.; Sivaraja, M. In *Advanced EPR: Applications in Biology and Biochemistry*; Hoff, A. J., Ed.; Elsevier: Amsterdam, 1989; pp 541−591.
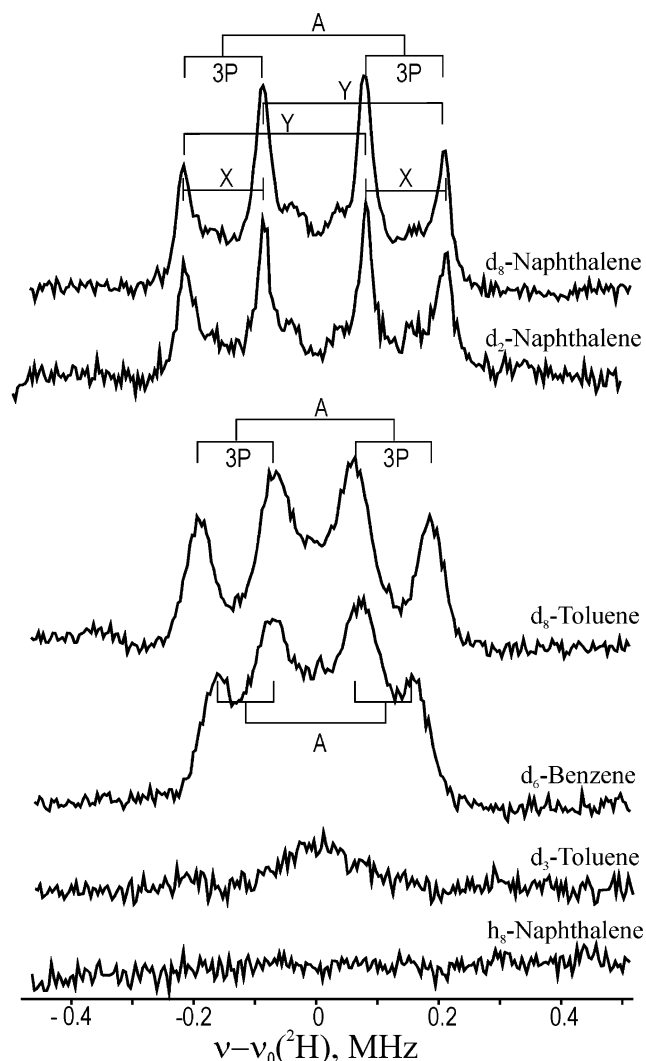
an Fe center involves three parameters: the polar and azimuthal Euler angles, $[\beta_A, \alpha_A]$, defined relative to the g-frame, for the Fe–D vector $\boldsymbol{r}_{Fe-D}$, and the length of that vector, r_{Fe-D}. Simulation for an axial quadrupole interaction (see below) similarly requires two Euler angles $[\beta_Q, \alpha_Q]$ and the value for the maximum splitting ($3P_{max}$). For the ring deuterons of an aromatic hydrocarbon, the value of $3P_{max}$ is known.[24−27] In this report, we determine the five remaining metrical parameters by simulations for a single deuteron (D1) of naphthalene. As discussed, these five parameters determine the location of D1 in the g-frame and the orientation of the C1−D1 bond. With this bond thus fixed, all permitted orientations of naphthalene can be generated by rotations about the C1−D1 bond. The five parameters of any other deuteron (here, D2 or D8) can be calculated as a function of this rotation angle (denoted as γ). We have used the bond lengths and bond angles of naphthalene to calculate the five simulations parameters for D2 and D8 of naphthalene, as a function of γ, using standard vector manipulations,[28] as implemented in Mathcad worksheets.

Results

EPR Spectra. NO−ferro−NDO exhibits an $S = {}^3/_2$ spin state.[7] The $S = {}^3/_2$ manifold is split into two doublets by an almost axial zero-field splitting interaction that is large, compared with the microwave quantum at 35 GHz; as a result, it exhibits an EPR signal only from transitions within the $m_s = \pm$ doublet. The signal from the substrate-free enzyme exhibits apparent g-values of $\boldsymbol{g} = [4.18, 3.88, 2.01]$, where g_3 corresponds to the unique axis of the zero-field splitting tensor; the splitting of g_1 and g_2 corresponds to a rhombicity of $\lambda = 0.025$. Binding of the substrate naphthalene causes a slight change in the g-values, to $\boldsymbol{g} = [4.21, 3.84, 2.01]$, and a sharpening of the spectrum. This suggests that the necessarily noncovalent binding of the substrate, as seen in the crystal structure of the indole adduct of ferro−NDO^R,[5] causes a slight reorganization of the active site, during which its structure becomes better defined.

Treatment of NO−ferro−NDO−[substrate] with dithionite leaves the signal from the non-heme-Fe center largely unchanged, although g_1 does change, from 4.21 to 4.25, while introducing a signal from the paramagnetic $[2Fe,2S]^{1+}$ state of the reduced Rieske center, with $\boldsymbol{g} = [2.01, 1.91, 1.74]$; we denote this reduced enzyme as NO−ferro−NDO^R. Because the breadth of the frozen-solution signal from the Fe−NO center is so much greater than that of the Rieske center, the appearance of the latter does not interfere with the collection of ENDOR spectra from the former at low fields. Conversely, the intensity from the Rieske center, with its narrow g-spread, is so much greater than that from the Fe−NO center that ENDOR signals collected at fields within the Rieske envelope are dominated by that center, even at fields where the two EPR signals overlap.

Mims ^{1,2}H-ENDOR at g_1 of NO−Ferro−NDO−[d_n-Substrate]. Figure 2 shows Mims single-crystal-like ^{2}H-ENDOR spectra collected at g_1 for adducts of NO−ferro−NDO with bound perdeuterated naphthalene, toluene, and benzene. All these spectra show the four-line pattern expected for the spectrum of a single deuteron, or set of equivalent deuterons,

(23) Hoffman, B. M.; DeRose, V. J.; Doan, P. E.; Gurbiel, R. J.; Houseman, A. L. P.; Telser, J. *Biol. Magn. Reson.* **1993**, *13*, 151−218.
(24) Barnes, R. G.; Bloom, J. W. *J. Chem. Phys.* **1972**, *57*, 3082−3086.
(25) Ragle, J. L.; Mokarram, M.; Presz, D.; Minott, G. *J. Magn. Res.* **1975**, *20*, 195−213.
(26) Ok, J. H.; Vold, R. R.; Vold, R. L.; Etter, M. C. *J. Phys. Chem.* **1989**, *93*, 7618−7624.
(27) Yim, C. T.; Gilson, D. F. R. *J. Phys. Chem.* **1991**, *95*, 980−983.
(28) Mathews, J.; Walker, R. L. *Mathematical Methods of Physics*; W. A. Benjamin, Inc.: New York, 1965.

Figure 2. Q-band Mims ^{2}H-ENDOR spectra at g_1 for NO−ferro−NDO bound with deuterated substrates as indicated. Conditions: microwave frequency, ~34.76 GHz; microwave pulse length ($\pi/2$), 52 ns; $\tau = 500$ ns; repetition rate, 100 Hz; spectral resolution, 256 points; 50 samplings of each point; $\cong$20 scans; RF pulse width, $T = 60\ \mu$s (naphthalene) and 20 μs (toluene, benzene).

of the substrate (eq 1). As indicated in Figure 2, such a spectrum is characterized by two splittings (X, Y): one which arises from the hyperfine coupling, and another which arises from the quadrupole interaction. X and Y are of comparable magnitude; therefore, one cannot immediately decide which should be assigned to the hyperfine interaction and which should be assigned to the quadrupole interaction. However, this issue is resolved by recognizing that the quadrupole splitting, $3P$, associated with any orientation has an upper bound of $3P_{max} = 3e^2qQ/2$ (in which the parameters have their usual definitions[29]), whose value is determined by the chemical bonding to the deuteron. For a deuteron bound to the ring of an aromatic hydrocarbon, the maximum quadrupole splitting is given as $3P_{max} \approx 270$ kHz.[24−27] The splitting is defined as $Y = 297$ kHz $> 3P_{max}$. Therefore, one must assign values of $3P = X = 131$ kHz and $A = Y = 297$ kHz; each of these numbers represents the arithmetic average of the two splittings (see Table 1). The

(29) Abragam, A.; Bleaney, B. In *Electron Paramagnetic Resonance of Transition Ions*, 2nd ed.; Dover Publications: New York, 1986; pp 436−442.

Table 1. ^{2}H-ENDOR Measurements at g_1 for
NO−ferro−NDO−[d_n-Substrate]

	d_2- and d_8-naphthalene		D(A)	
	D1(A)	D1(B)	d_8-toluene	d_6-benzene
A/kHz ^{a}	297	200	251	230
$3P$/kHz ^{a}	131	127	121	88
$3P_{max}$ ^{a}	265.1 (2.3)		269.9 (2.6)	271.1 (2.3)
ψ ^{b} (eq 2)/degrees	86	83	80	70

^{a} $3P_{max} = 3e^2qQ/2$ (from ref 24). ^{b} Errors in splitting, A and $3P$, are $\sim$15 kHz; error in ψ is 10°.

substrate cannot covalently bond to the metal center; therefore, this hyperfine coupling must arise from the through-space dipolar interaction between the electron spin and the substrate deuteron.

This assignment of the splittings is confirmed by subtracting a ^{1}H ReMims pulsed ENDOR spectrum taken at g_1 for d_8-naphthalene from one for h_8-naphthalene. The difference spectrum shows a doublet, with $A(\text{H}) = 1.93$ MHz, that is lost upon deuteration, precisely corresponding to the deuteron hyperfine splitting when multiplied by the ratio of nuclear g-factors (6.51) (see figures given in the Supporting Information).

The peaks in the NO−ferro−NDO−[d_8-naphthalene] spectrum are very sharp, with widths of $\sim$30 kHz. Such sharp lines first imply that the naphthalene molecule adopts a very well-ordered binding geometry in the substrate pocket. Second, these peaks indicate that *both* the quadrupole and hyperfine couplings must be near extrema values, as follows. Although an ENDOR spectrum collected at g_1 of a frozen-solution sample is single-crystal-like, with the external field lying approximately along the g_1 molecular axis, even such a spectrum inevitably arises to some degree from a distribution in orientations of the field relative to the *g*-frame, as a result of the breadth in field of the exciting microwave pulse and the existence of a nonzero EPR component line width. For arbitrary relative orientations of hyperfine or quadrupole interaction tensors, with respect to the *g*-frame, the different members of this distribution will have different values for the hyperfine and quadrupole interactions. Only when an interaction is near an extremum would all members of this distribution have essentially the same interaction constant, and such narrow ENDOR lines could be observed only if this is true for the hyperfine *and* quadrupole contributions. Finally, the sharpness suggests that the pattern comes from a single deuteron, not two deuterons, which would have to be accidentally symmetry-equivalent to give identical, overlapping spectra.

Because the quadrupole coupling is located at an extremum, we can use the spectrum collected at g_1 to estimate the relative orientation of the C−D bond vector and the g_1-direction. First, the quadrupole interaction of an aromatic deuteron has axial symmetry, with reference values of $3P_{max}$ given in Table 1.[24] Second, the nuclear Zeeman splitting dominates both hyperfine and quadrupole interactions: $\nu_D \gg A$ and $3P$. Under these conditions, the quadrupole splitting obeys the relationship

$$3P = \left|3P_{max}\left(\frac{3\cos^2\psi - 1}{2}\right)\right| \qquad (2)$$

Here, ψ is the angle between the unique axis of the quadrupole tensor and the external magnetic field; for the single-crystal-

like spectrum in Figure 2, the field lies along the g_1-direction, and, thus, ψ corresponds to the angle between the C−D bond vector and the g_1-axis. For enzyme-bound d_8-naphthalene, the average splitting at g_1 is $3P = 131$ kHz (Table 1); use of the reference value, $3P_{max} = 265$ kHz,[24] yields ψ values of $\sim$35° or $\sim$86°. The requirement that the coupling be near an extremum requires the choice $\psi \approx 86°$, corresponding to the "perpendicular" extremum at $\psi = 90°$. This calculated angle is corroborated by the analysis of 2-D, orientation-selective ENDOR patterns, presented below.

Next, consider the hyperfine interaction. The hyperfine coupling to nuclei of a substrate that is adjacent to a metal center, but not coordinated to it, arises from the through-space dipolar interaction between the electron and nuclear spins.[21,30,31] With this interaction near an extreme for the g_1 spectrum, as indicated by the sharp lines, the Fe−D vector must lie either along or perpendicular to the g_1-direction. The *intrinsic* coupling to $S = {}^3/_2$ spin of the Fe ion would then have the magnitude $A = (g_e/g_1)A' = 2T$ or $A = T$ for the g_1 spectrum,[32] where

$$T = \frac{\rho_{Fe}g_e\beta_e g_D\beta_D}{r_{Fe-D}^3} \qquad (3)$$

Here, ρ_{Fe} is the electron spin density on Fe; g_e, β_e, g_D, and β_D have their usual meanings, and r_{Fe-D} is the Fe−D(A) distance. For ρ_{Fe} values close to unity (see below), the observed value, $A' = 297$ kHz, yields $r_{Fe-D} \approx 4.4$ Å for an Fe−D(A) vector approximately perpendicular to the g_1-direction, quite compatible with the distance found for indole bound in the substrate pocket,[5] and a rather longer distance of $r_{Fe-D} \approx 5.6$ Å if the vector is taken parallel to the g_1-direction. Confirmation that this vector indeed lies approximately perpendicular to the g_1-direction, with $r_{Fe-D} \approx 4.3$ Å, comes in the discussion given below, through analysis of the 2-D ENDOR pattern.

To distinguish whether the D(A) deuteron that gives rise to the quartet in the g_1 spectrum of NO−ferro−NDO−[d_8-naphthalene] is D1 or D2 of naphthalene, we examined NO−ferro−NDO with bound di-deutero-naphthalene, naphthalene D1, D4; Figure 2 presents a g_1 Mims ENDOR spectrum from this sample. The quartet pattern observed for NO−ferro−NDO−[d_8-naphthalene] is preserved with the d_2 substrate. A quartet from the sample with d_2-naphthalene must arise from a single D1 deuteron; therefore, it follows that the quartet in the spectrum with the d_8-naphthalene substrate similarly arises. The lines in the spectra for d_2-naphthalene appear somewhat narrower than those for d_8-naphthalene. We confirm below that the sharpening does not come from the loss of an almost-equivalent, D2 deuteron signal.

The spectrum of the d_8-naphthalene adduct further shows weaker features that, as indicated in Figure 2, comprise a four-line pattern from a second deuteron, D(B), of the substrate. These features persist in the spectrum taken from the sample prepared with di-deutero-naphthalene (Figure 2); thus, they do not represent a signal from the more-remote D2/D8 deuterons. Instead, we must assign D(B) to a minority conformation of bound naphthalene. This "D1(B)" pattern exhibits essentially

(30) Tierney, D. L.; Huang, H.; Martasek, P.; Roman, L. J.; Silverman, R. B.; Hoffman, B. M. *J. Am. Chem. Soc.* **2000**, *122*, 7869−7875.
(31) Tierney, D. L.; Huang, H.; Martásek, P.; Masters, B. S. S.; Silverman, R. B.; Hoffman, B. M. *Biochemistry* **1999**, *38*, 3704−3710.
(32) We have reinserted the prime here for clarity.

the same quadrupole splitting as that observed for the first deuteron (D1 = "D1(A)"), $3P(B) = 127$ kHz, which corresponds to a similar angle between the C−D1(B) vector and the g_1-axis (Table 1). The hyperfine coupling is smaller, $A(B) = 200$ kHz. According to eq 3, this suggests a greater Fe−D1 distance, with a distance ratio of $r_{Fe−D}(B)/r_{Fe−D}(A) \approx (297\ kHz/200\ kHz)^{1/3} \approx 1.14$, or $r_{Fe−D}(B) \approx 5$ Å, for $r_{Fe−D}(B)$ perpendicular to the g_1-direction.

Spectra for NO−ferro−NDO with bound d_8-toluene and d_6-benzene similarly show a deuteron quartet pattern (Figure 2). In the deuteron pattern of d_8-toluene, both the quadrupole and hyperfine couplings are slightly smaller than those of the D1-(A) deuteron of d_8-naphthalene; the d_8-toluene quadrupole value of $3P = 121$ kHz corresponds to a similar value of ψ, which is the angle between the C−D vector and the g_1-axis (Table 1). The hyperfine coupling for d_6-benzene is slightly smaller, yet its quadrupole splitting is appreciably smaller (Table 1). The line widths *appear* to increase (naphthalene < toluene ≤ benzene); however, this observation is, in large part, because, to get equivalent signal/noise in all these spectra, those with d_8-toluene and d_6-benzene were taken with shorter RF pulse widths ($T = 20\ \mu s$ rather than $60\ \mu s$) and, thus, RF bandwidths that are ∼3 times greater. (We illustrate the resulting line-broadening below by presenting paired spectra for d_8-toluene as the substrate, taken at the two different pulse widths.)

The ^{2}H-ENDOR quartet lines seen at g_1 for NO−ferro−NDO−d_8-toluene is abolished when the complex is prepared with methyl-d_3-toluene; instead, one sees only a weak "distant" ENDOR signal near the ^{2}H Larmor frequency at g_1 (Figure 2) and all other g-values. This indicates that the deuteron quartet for d_8-toluene comes from a ring deuteron, and that the methyl group of bound toluene is directed *away* from the Fe−NO center.

Orientation-Selective ^{2}H-ENDOR Spectra of NO−Ferro−NDO−[d_n-Naphthalene] ($n = 2, 8$). To fully define the naphthalene binding geometry, we generated 2-D field-frequency plots that were comprised of multiple Mims ^{2}H-ENDOR spectra collected across the EPR envelope for NO−ferro−NDO with bound di-deutero-naphthalene (Figure 3) and for NO−ferro−NDO-[d_8-naphthalene] (Figure 4). We also collected and simulated the corresponding 2-D ^{2}H-ENDOR patterns (see Supporting Information) for NO−ferro−NDO with substrates d_8-toluene and d_6-benzene. As seen with some other systems where $S > 1/2$, the electron spin−echo (ESE) signal becomes too weak to collect spectra at fields higher that g_2,[30] but, aided by the analysis of the g_1 spectra, it is nonetheless possible to simulate the 2-D data.
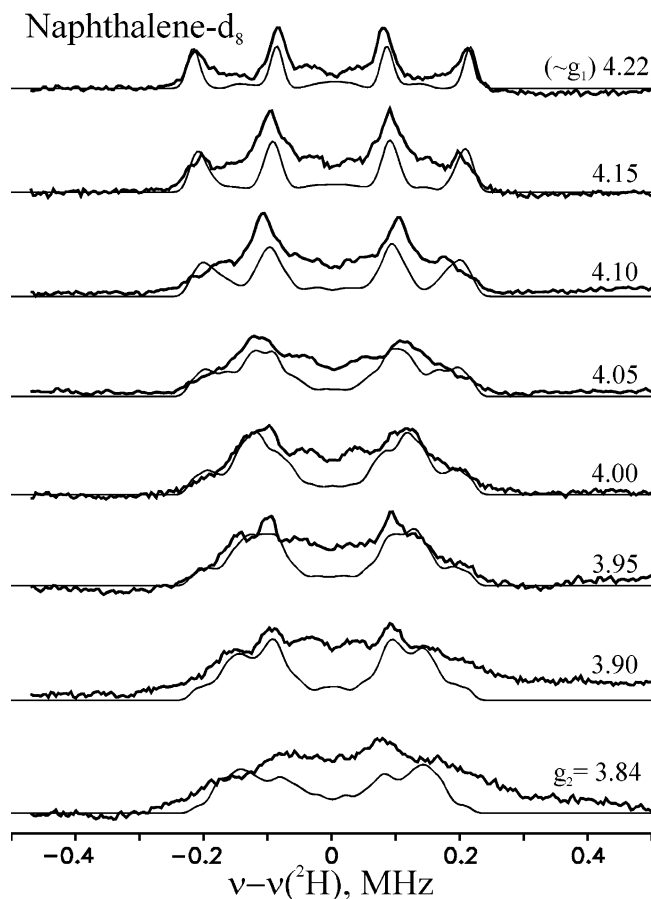
2-D ENDOR Pattern for D1 from NO−Ferro−NDO−[D1,D4-Naphthalene]. The D(A) g_1 ^{2}H-ENDOR spectra of Figure 2 were interpreted in the previous discussion in terms of the response from a bound naphthalene whose D1 deuteron most likely lies approximately perpendicular to the g_1-direction, and whose C−D1 vector also is perpendicular to the g_1-direction ($\psi \approx 85°$, with respect to the g_1-axis). We employed this starting point to analyze the 2-D ENDOR pattern for D1 of NO−ferro−NDO−[D1,D4-naphthalene] (Figure 3). The simulations, which followed procedures that have been described elsewhere,[23] independently varied the orientations of the quadrupole and the hyperfine tensors, relative to the *g*-tensor. The final simulations given in Figure 3 beautifully reproduce the data.
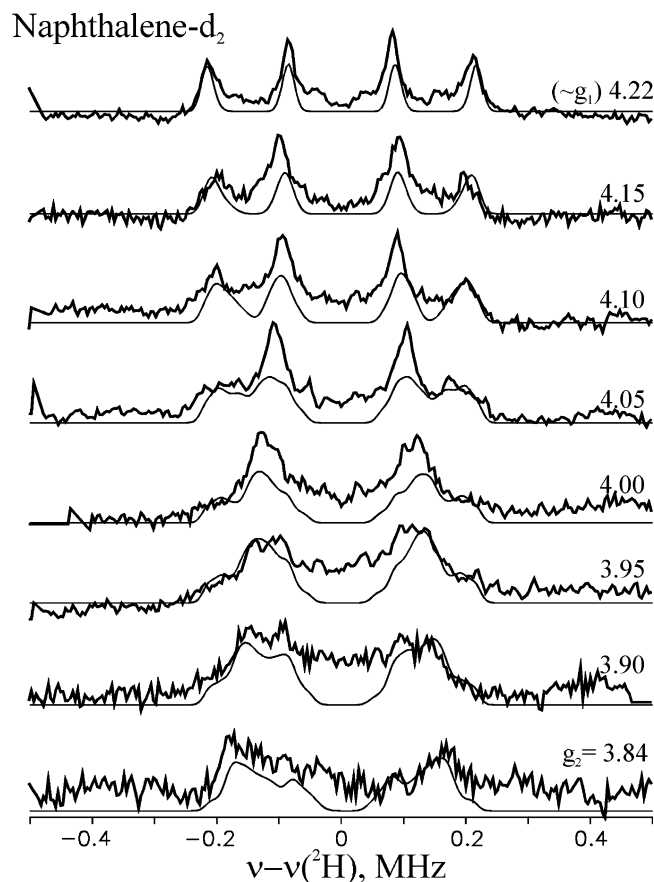
Figure 3. Q-band 2-D Mims ^{2}H-ENDOR spectra of NO−ferro−NDO−[d_2-naphthalene]; bold lines represent experimental data and thinner lines represent simulated data. The simulated ENDOR and EPR line widths are 30 kHz and 400 MHz, respectively, and spin Hamiltonian parameters are listed in Table 1.

Regarding the quadrupole interaction, as previously discussed, the quadrupole tensor for a ring deuteron of these substrates has axial symmetry around the C−D bond with the unique (largest) tensor component, $3P_{max}$ (Table 1), pointing along the C−D bond; in general, the quadrupole coupling is further characterized by an asymmetry parameter, η, but this is negligible for C−D ($\eta \leq 0.05$). Defining the C−D bond as lying along the P_3-direction of the quadrupole principal-axis frame, the quadrupole-tensor components in this frame are $\boldsymbol{P} = [−P_{max}/2, −P_{max}/2, P_{max}]$. P_{max} is known (Table 1), so the only quadrupole parameters to be fit are the two Euler angles relating $\boldsymbol{P}$ to the *g*-frame, $[\alpha_Q, \beta_Q]$, where the latter is the polar angle; the fitting procedure is initiated with the condition that the C−D1 bond makes an angle of $\psi \approx 85°$, or less likely ∼35°, with respect to the g_1-axis, where $\cos \psi = \sin(\beta_Q) \cos(\alpha_Q)$. The best simulation corresponds to $\psi \approx 85°$; in fact, simulations with $\psi \approx 35°$ give broadened peaks at g_1, as expected. The actual Euler angles relative to the *g*-tensor, given in Table 2, place the C−D1 bond in the $g_2−g_3$ plane at an angle of $\beta_Q = 45°$, or $\beta_Q = 180° − 45° = 135°$, with respect to the g_3-axis. The former value would "clash" the naphthalene ring(s) with atoms of the Fe coordination sphere, and, thus, the latter must correspond to the orientation of the naphthalene molecule, with respect to the metal ion. (See below.)

The simulations for D1(A) (Figure 3) employ the hyperfine parameters given in Table 2. The hyperfine interaction is

Naphthalene-d$_8$

$(\sim g_1)$ 4.22

4.15

4.10

4.05

4.00

3.95

3.90

g_2= 3.84

$-0.4 \qquad -0.2 \qquad 0 \qquad 0.2 \qquad 0.4$

$\nu-\nu(^2H)$, MHz

Figure 4. Q-band 2-D Mims ^{2}H-ENDOR spectra of NO−ferro−NDO−[d$_8$-naphthalene]; bold lines represent experimental data and thinner lines represent simulated data. The simulated ENDOR and EPR line widths are 30 kHz and 400 MHz, respectively, and spin Hamiltonian parameters are listed in Table 1.

Table 2. ^{2}H-ENDOR Simulation Parameters for NO−ferro−NDO−[d$_n$-Substrate]

	d$_2$- and d$_8$-naphthalene	d$_8$-naphthalene		D(A)	
	D1	D2	D8	d$_8$-toluene	d$_6$-benzene
T^a/kHz	142	91	77	133	133
Euler angles [α, β]^b/degrees					
hyperfine	[60,10]	[15,20]	[20,30]	[45, 15]	[30, 15]
quadrupole	[90,45]	[15,65]	[90,45]	[70, 50]	[65, 50]
$r_{Fe−D}$ (Å)^c	4.3	5.0	5.3	4.4	4.4

^{a} $T = \rho_{Fe}g_e\beta_eg_D\beta_D/r^3$. The error in T is approximately ±10 kHz; calculations employed a ρ_{Fe} value of 0.95. ^{b} For both the hyperfine and quadrupole interactions, β is the standard polar angle, relative to the g_3-direction, and α is the azimuthal angle, measured relative to the g_1-direction. The errors in the Euler angles α and β are approximately ±10°. ^{c} Precision of $r_{Fe−D}$ is +0.1 Å.

traceless, supporting the expectation that the D1 hyperfine interaction involves only a through-space dipolar coupling between the electron spin of the $S = ^3/_2$ NO−ferrous center and the ^{2}H atom of the substrate, with no isotropic component from Fe−substrate bonding. Furthermore, the finding of an *intrinsic* hyperfine interaction that has the form of a simple point−dipole coupling between a nucleus and a single center of electron spin $A = [−T, −T, 2T]$ indicates that the coupling is dominated by spin located on the Fe atom. If the dipolar interaction between a nearby nucleus and the Fe−N−O center included major contributions from spin delocalized onto N and/

Chart 1
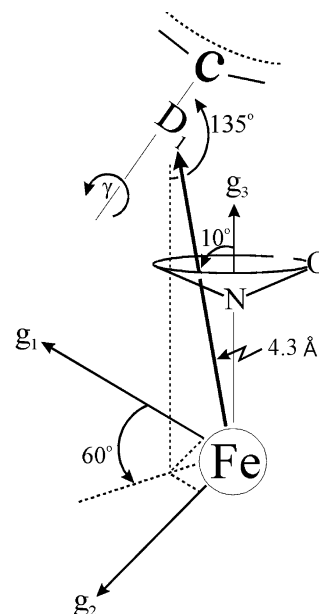
or O, the interaction matrix could not have this simple form.[33] This picture is further supported by the ^{14}N ENDOR results discussed below. For a point−dipole interaction, T is given by eq 3, and the unique hyperfine value ($2T$) points along the Fe−D1 vector. The Euler angle, β_A, for the hyperfine tensor is defined as the angle between the $r_{Fe−D}$ vector and the g_3-direction (which corresponds to the unique zero-field splitting axis of the true, $S = ^3/_2$, electron-spin system), whereas the azimuthal angle is defined as a rotation about the g_3-axis, away from the g_1-direction; these definitions are the same as for the axially symmetric quadrupole interaction. The fits give $\beta_A \approx$ 10°, placing the Fe−D1 vector close to the g_3-direction, as anticipated previously.

From eq 3, a calculation of $r_{Fe−D}$ from an experimentally determined value of T requires a value for the spin density on the Fe atom. Similar to prior work on hemes,[31] we take ρ_{Fe}. ≈ 0.95. Fortunately, the dependence on ρ_{Fe} is weak: $r_{Fe−D}$ $= (\rho_{Fe}g_e\beta_eg_D\beta_D/T)^{1/3}$. The Fe−D1 distance thus calculated is 4.3 Å; this can be considered as an upper bound, in that the effect of including any contribution from small amounts of spin density on NO would be to shorten $r_{Fe−D}$. The disposition of D1 and the C−D1 bond, relative to the g-frame, are shown in Chart 1. Similar distances are found for the other substrates (see Table 2).

2-D Pattern for NO−Ferro−NDO−[d$_8$-Naphthalene]. Comparison of the 2-D patterns for d_2-naphthalene (Figure 3) and d_8-naphthalene (Figure 4) shows an overall loss of resolution in the latter, as well as the loss of additional intensity at certain frequencies and fields, all of which is attributed to the elimination of the ENDOR response of the adjacent D2/D8 deuterons. In the absence of well-defined features that could be cleanly assigned to this deuteron, we used the available geometric constraints to define the naphthalene geometry. With the position of D1[34] in the g-frame, as well as the orientation of C−D1, having been determined previously from the d_2-

(33) DeRose, V. J.; Liu, K. E.; Lippard, S. J.; Hoffman, B. M. *J. Am. Chem. Soc.* **1996**, *118*, 121−134.
(34) All simulations of 2-D patterns refer to the A binding site; therefore, we have dropped the A/B notation, unless needed.
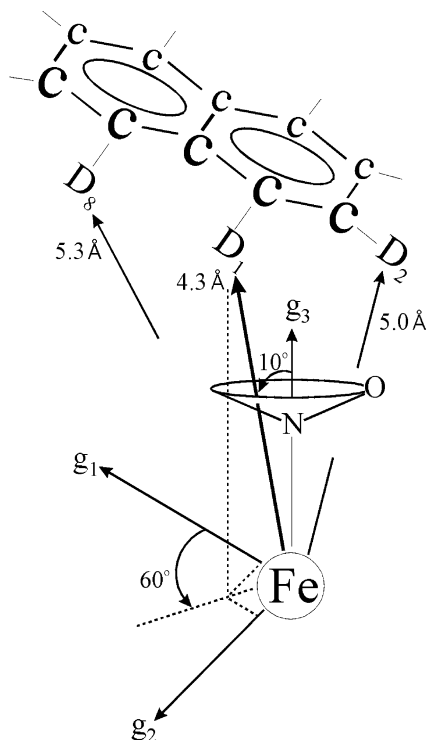
Figure 5. ENDOR-derived geometry of naphthalene bound to NO−ferro−NDO.

naphthalene sample, then all possible orientations of naphthalene itself, and thus of D2 and D8, can be generated by a rigid-body rotation of naphthalene about the C−D1 bond. The angle of rotation, γ, in Chart 1 is defined such that $\gamma = 0$ corresponds to a zero dihedral angle between the naphthalene and the g_1−g_2 planes. The constraint that neither D2 nor D8 can be closer to the Fe atom than D1 (or closer than ∼4 Å) is needed to avoid steric clash, which limits the rotation around C−D1 to γ values of ∼0°−10° or ∼170°−190°, leaving an essentially binary choice of orientations for naphthalene about the C−D1 bond. The hyperfine and quadrupole parameters for D1 and D8 for these values of γ are then fully determined by the structure of naphthalene and the value of γ. (See Materials and Methods section.) The final choice of $\gamma \approx 190°$, corresponding to the structure shown in Figure 5, is required if the naphthalene is to fit into the pocket occupied by indole. It places D1, D2, and D8 as indicated in the figure; D1 is closest to the Fe atom (∼4.3 Å), D2 is farther away (∼5.0 Å), and D8 is farther yet (∼5.3 Å). Considering that the contributions from D2 and D8 are entirely fixed by the simulation for D1 and (parametrically) by the value of γ, rather than by independent fitting, we consider the resulting simulations to be extremely satisfactory (Figure 4); the simulation parameters are listed in Table 2.

Mims ²H-ENDOR of NO−Ferro−NDOR−[d_n-Substrate]. The binding of oxygen is coupled to both the binding of the substrate and the reduction of the Rieske center; therefore, we used ²H-ENDOR of the NO−ferro analogue to test for the possibility of an allosteric shift in the substrate position upon reduction of the Rieske center.[14] Figure 6 displays absolute ²H-ENDOR spectra of d_8-naphthalene collected at g_1 for NO−ferro−NDOR−[d_8-naphthalene], as well as for NO−ferro−NDO−[d_8-naphthalene]. Both spectra show the four-line patterns of D1(A) and D1(B). However, the intensity of the D1(B)
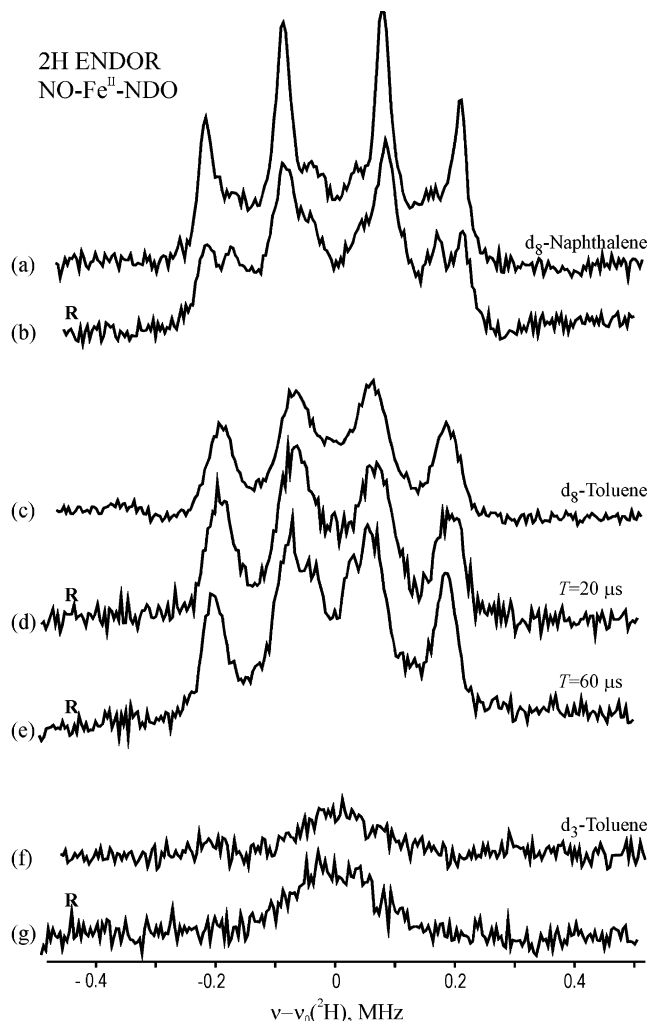

Figure 6. Q-band Mims ²H-ENDOR spectra at g_1 for NO−ferro−NDOR bound with deuterated substrates as indicated. Conditions are same as those in Figure 1, except that RF = 60 μs for spectra a, b, and e, and RF = 20 μs for spectra c, d, f, and g.

Chart 2
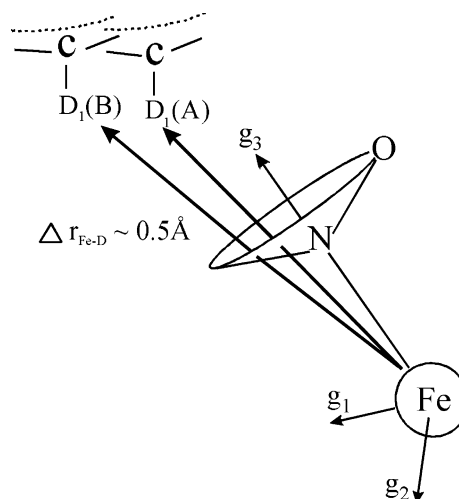
pattern is greatly enhanced in the NDOR spectrum, indicating the occurrence of an allosteric shift from A to B binding geometries/sites, corresponding to a motion of ca. 0.5 Å upon reduction of the Rieske center, as indicated in Chart 2; spectra at other g-values, although of lower resolution, confirm this
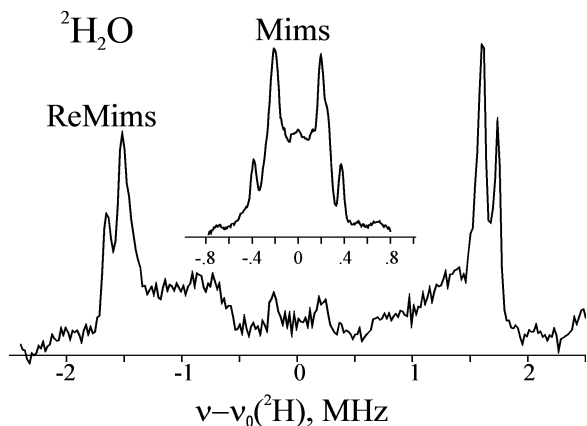
Figure 7. Q-band ^{2}H-ENDOR spectra of NO−ferro−NDO-[h_8-naphthalene] in D$_2$O solution acquired by applying Re-Mims (bottom), and Mims (same conditions as those listed for Figure 1) pulse sequences. The conditions in Re-Mims ENDOR are as follows: $\tau_1 = 144$ ns; $\tau_2 = 400$ ns; repetition rate, 100 Hz; spectral resolution, 256 points; 50 samplings of each point; 20 scans.

conclusion. The total intensities of the NDO and NDO^R spectra are approximately the same, which indicates that reduction does not shift naphthalene from the A- and B-sites to a third, more distant site.

Figure 6 also compares absolute ENDOR spectra of NO−ferro−NDO and NO−ferro−NDO^R with bound d_8-toluene and methyl-d_3-toluene. The ($T = 20$ μs) deuteron quartet for d_8-toluene shows no difference upon reduction of the Rieske center; correspondingly, bound d_3-toluene does not acquire a resolved deuteron quartet upon reduction. Thus, toluene binds near to the Fe atom with the ring pointing toward the Fe atom, with the nearest ring deuteron at a distance $r_{Fe−D} \approx 4.4$ Å; the methyl group points away from the Fe atom, regardless of the oxidation state of the Rieske center. The conservation of absolute ENDOR intensity in the two spectra again shows that reduction of the Rieske center does not shift this substrate to a more remote site.

Figure 6 also shows a spectrum from NO−ferro−NDO^R−[d_8-toluene], taken using $T = 60$ μs. The comparison of spectra taken from NO−ferro−NDO^R using $T = 20$ and 60 μs show that the ENDOR signals collected with the larger RF bandwidth ($T = 20$ μs) are broadened. (Unfortunately, sensitivity considerations precluded using this pulse width for the NO−ferro−NDO-[d_8-toluene]; however, it too can be assumed to have narrower intrinsic lines.) The higher-resolution, $T = 60$ μs spectrum for NO−ferro−NDO^R−[d_8-toluene] shows resolved features near the deuteron Larmor frequency that could either be associated with D2 and/or D8 on the same substrate, or a second nearby site; the absence of a $T = 60$ μs spectrum for a sample with the oxidized Rieske cluster precludes a conclusion.

For completeness, we looked for ^{2}H-ENDOR signals associated with the EPR signals from the reduced Reiske center. None were observed.

ENDOR of Water Deuterons. The structure of the ferro−NDO^R complexes exhibits a water bound to the Fe atom (denoted as WAT1). The Re-Mims pulsed ENDOR signal at g_1 for NO−ferro−NDO−(h_8-naphthalene) in D$_2$O solution exhibits a doublet of quadrupole doublets with hyperfine coupling, A'-(D) $= 3.5$ MHz, corresponding to A'(H) $= 22.8$ MHz. (See Figure 7.) This corresponds to an intrinsic value of A(H) $= 10.83$ and must arise from bound water. We collected 2-D Mims ^{2}H-

ENDOR of the WAT1 deuteron over the field range, $g_1 = 4.21$ to $g_2 = 3.84$ (not shown), and simulated the patterns to obtain hyperfine and quadrupole interaction parameters. For the water ligand, WAT1, the hyperfine tensor is not traceless but rather has an isotropic contribution, which confirms that this signal is associated with a water bound to an Fe atom. Thus, WAT1 is not lost either upon the binding of NO to ferro−NDO, or upon the binding of O$_2$ to ferro−NDO^R, as seen by X-ray.

A second ^{2}H-Mims signal, with A'(D) $= 597$ kHz, is provisionally assigned to WAT2, a second water revealed by the ferro−NDO−indole crystal structure that lies $\sim$3.5 Å away from the Fe atom and is hydrogen-bonded to Asp362. (The next-closest exchangeable proton is from a third water, which is $\sim$4.2 Å away from the Fe^{2+} cation, and may contribute to the intensity with even smaller couplings in the center of the spectrum.) Analysis of a 2-D ^{2}H-ENDOR pattern for WAT2 shows that, here, the hyperfine interaction is purely dipolar, as expected, on the basis of its large distance from the Fe atom in the Fe−NDO structures;[4,5] the value, $T = 272$ kHz, corresponds to a distance of $r_{Fe−D} \approx 3.5$ Å in NO−ferro−NDO−[d_8-naphthalene].

ENDOR of ^{14}N. The NO−ferro−NDO−substrate adducts show a rich ^{14}N-ENDOR response at g_1, with a maximum frequency of $\nu \approx 12$ MHz and features extending to lower frequencies (data not shown); taking into account quadrupole effects and the ^{14}N nuclear Larmor frequency, this corresponds to a maximum in the *observed* hyperfine couplings of $A' \approx 20$ MHz and, thus, a maximum *intrinsic* coupling of $A = (g_e/g_1)A'$ ≈ 10 MHz. Without isotopic labeling, it is not possible to assign particular features to the two different histidine ligands disclosed by the X-ray crystal structure, plus the N atom of NO. However, the size of the coupling is similar to that which we have measured for ^{14}N ligands to non-heme Fe centers, supporting our treatment of the deuteron couplings.[35] We note that this interpretation has implications for the electronic structure of Fe−NO that will be the subject of further investigation. There are numerous possible interpretations of the electronic structure of the $S = {}^3/_2$ Fe−NO fragment.[36] The most popular interpretation is that it is describable as Fe^{3+}−(NO)$^-$, with a high-spin ($S = {}^5/_2$) ferric ion antiferromagnetically coupled to a "high-spin" ($S = 1$) NO anion.[20] However, such a model would not lead to a simple point−dipole interaction with deuterons of the substrate (see previous discussion); thus, the ENDOR results instead suggest that it is better to treat the fragment in terms of an intermediate spin ($S = {}^3/_2$) ferric ion with a diamagnetic (NO)$^-$ ligand. We note, however, that the bond between Fe and NO can be viewed as resulting from spin pairing between an odd electron on Fe^{2+} and the odd electron on NO•, and, as we have discussed, a variety of interpretations can be placed on such a bond.[37]

Discussion

High-resolution Mims ^{2}H-ENDOR spectra have been recorded for the NO−ferrous center of the non-heme enzyme

(35) Rocklin, A. M.; Tierney, D. L.; Kofman, V.; Brunhuber, N. M. W.; Hoffman, B. M.; Christoffersen, R. E.; Reich, N. O.; Lipscomb, J. D.; Que, J. L. *Proc. Natl. Acad. Sci. U.S.A.* **1999**, *96*, 7905−7909.
(36) Westcott, B. L.; Enemark, J. H. In *Inorganic Electronic Structure and Spectroscopy*, Vol. 2; Solomon, E. I., Lever, A. B. P., Eds.; Wiley: New York, 1999; pp 403−450.
(37) Summerville, D. A.; Jones, R. D.; Hoffman, B. M.; Basolo, F. *J. Chem. Educ.* **1979**, *56*, 157−162.

naphthalene dioxygenase (NDO) bound with substrates d_8-naphthalene, d_2-naphthalene, d_8-toluene, d_3-toluene, and d_6-benzene. Samples were prepared in a D_2O buffer, to test for solvent-derived ligands. Spectra were collected from the enzyme, with the Rieske diiron center in both its oxidized (NDO) and reduced (NDO^R) states.

Naphthalene as the Substrate. The ^2H spectra collected at g_1 from NO–ferro–NDO–[d_n-naphthalene] ($n = 2, 8$) show a sharp ^2H quartet from the D1 of naphthalene in the majority A binding geometry (Figure 2). The hyperfine tensor for the A-site D1 was determined by analysis of orientation-selective, 2-D ENDOR patterns collected for the d_2-naphthalene sample (Figure 3). The results define the location of the D1 deuteron, with respect to the *g*-frame of the iron center, showing it to lie 4.3 Å from the Fe atom, slightly off the g_3-axis; in addition, the determination of the D1 quadrupole tensor disclosed the *orientation* of the C–D1 vector, with respect to the **g**-tensor frame (see Chart 1).

With this starting point, we were able to interpret the orientation-selective, 2-D ENDOR pattern collected from NO–ferro–NDO–[d_8-naphthalene] (Figure 4). Additional intensity in the 2-D patterns of perdeuterated naphthalene, as compared to the di-deutero substrate, reflects intensity from the D2/D8 deuterons; however, the extra intensity is not resolved well-enough to permit direct analysis. Instead, we considered geometries allowed for naphthalene binding, subject to the geometric constraints for D1 that are summarized in Chart 1. These considerations, supported simulations of orientation-selective, 2-D ENDOR patterns for the perdeuterated naphthalene sample that summed contributions from D1/D2/D8, led to the ENDOR-derived geometry of the A-site naphthalene and Fe–NO fragment that is presented in Figure 5. As shown, D1 is ~10° off the g_3-axis, which must lie along the Fe–NO bond, because this bond represents the dominant interaction at the Fe atom. The two deuterons of the reactive carbons, D1 and D2, are closest to the Fe atom ($r_{Fe–D1} = 4.3$ Å, $r_{Fe–D2} = 5.0$ Å), whereas D8 is farther away ($r_{Fe–D8} = 5.3$ Å) (see Figure 5). Perhaps more instructive, the D1–N(O) and D2–N(O) distances are ~2.4 and ~3.3 Å, respectively, whereas the D8–N distance is ~3.7 Å. The figure does not specify where the O atom of NO lies, because we have no evidence regarding this question. However, we expect that the g_1- and g_2-axes also are oriented by the Fe–NO bonding interactions, and that one of these axes is likely to lie perpendicular to this Fe–N–O plane, whereas the other lies parallel to it.

This proposed structure is completely consistent with the crystal structure of the ferro–NDO^R–indole adduct,[5] as well as that of the recently reported ferro–NDO^R–naphthalene adduct.[13] The pyrrole ring of indole points "inward" toward the Fe, and the benzene ring points "outward", toward the pocket entrance; naphthalene assumes essentially the same orientation. The indole proton closest to the Fe^{2+} cation is ~4.2 Å away, whereas the C1 proton of naphthalene is ~3.8 Å away. These distances are similar to, but ~0.7–1.1 Å shorter than, the value we have estimated here for the distance between the Fe atom and the naphthalene C1 proton in the NO–ferro–NDO^R–naphthalene complex (~4.9 Å). A recent crystallography study also provides the first structure of an oxy-adduct of the NDO^R–indole complex. Both the crystal structure and the current spectroscopic study show that there is ample room for binding

dioxygen to the Fe atom of a substrate adduct without major rearrangement of the catalytic site, and that dioxygen could readily attack the reactive atoms of the aromatic ring. Significantly, the crystal structure shows that the angle between the proximal Fe–O bond of the oxy-complex and the C1 proton of indole is ~13°, which completely agrees with the angle between the Fe–N bond and the naphthalene C1 proton of 10° that has been determined here. Thus, NO appears to be a good surrogate for O_2 in this system, whereas the X-ray structures of complexes formed *in crystals* are seen to be in accord with structural information derived from enzymes frozen after making complexes *in solution*.

The ENDOR spectra of solvent-exchangeable deuterons show that the water of ferro–NDO is retained upon binding NO (Figure 7); thus, the model of Figure 5 suggests that NO, and presumably O_2, bind by *addition* to the five-coordinated ferro–NDO, again in accordance with the recent structure.[13]

Binding Geometry of Toluene and Benzene. Each of these two perdeuterated substrates shows a ^2H pattern dominated by a single-ring deuteron with many of the same spin Hamiltonian parameters as D1 of naphthalene. Thus, for these substrates, the position of this ring deuteron and the orientation of its C–D bond are not appreciably different from those for D1 of A-site naphthalene. Hence, the single ring of toluene and of benzene adopt much of the same position as the "proximal" ring of the bound naphthalene (Figure 5).

It is surprising to find that the toluene molecule in the substrate pocket is oriented with the ring "toward the Fe atom"; the methyl group is pointing away from it. Although toluene dioxygenase catalyzes toluene to *cis*-toluene dihydrodiol by incorporating an oxygen molecule into the benzene ring,[38] the only products of toluene oxidation by NDO are benzyl alcohol and benzaldehyde, which are products that result from reaction with the methyl group, not the ring.[11] Similarly, although we find that benzene binds in the active site of NDO in a position comparable to that of the naphthalene ring that is oxidized during turnover, very little benzene *cis*-diol product is produced in turnover reactions. Instead, uncoupling occurs to generate hydrogen peroxide as the dominant product. These discrepancies between the observed binding geometry and those anticipated for both toluene and benzene may indicate that changes in active site geometry and/or the binding position of the substrates occur dynamically during the catalytic cycle. As we now discuss, the current study in fact provides the first evidence for structural changes that depend on the redox state of the Rieske cluster.

Allosteric Influences of Rieske Center Reduction. Although ferro–NDO and ferro–NDO^R both possess mononuclear iron sites that could, in principle, react with O_2 to yield reactive oxygen species, neither does so at a high rate in the absence of a substrate. Substrate binding appears to provide the trigger to allow O_2 to become activated and subsequently react in almost 100% yield with the nearby substrate. Structural comparisons between samples with oxidized and reduced Rieske clusters have not previously been made because the Rieske cluster is reduced in the X-ray beam, and thus the present results provide the first suggestions in regard to the mechanism of this activation.

We have found that reduction of the Rieske center allosterically decreases the population of the "A" naphthalene binding

(38) Ziffer, H.; Jerina, D. M.; Gibson, D. T.; Kobal, V. M. *J. Am. Chem. Soc.* **1973**, *95*, 4048–4049.

conformation, which dominates when the cluster is oxidized, and in which the closest deuteron is ca. 4.3 Å from the Fe atom.[14] Reduction shifts the substrate binding toward the "B" conformation, ~0.5 Å farther away from the Fe atom than that in the A conformation (Chart 2); the sum of the populations (ENDOR intensities) of the two conformations appears unchanged by reduction, indicating that reduction does not also shift naphthalene from these two "close" binding sites to more-distant sites.

The crystal structure of NDO^R makes it seem reasonable that structural changes caused by reduction of the Rieske cluster might be transmitted to the mononuclear iron center. The quaternary structure of reduced NDO links the Rieske cluster of one α-subunit to the mononuclear iron in the adjacent α-subunit 12 Å away: the active-site mononuclear Fe atom of one α-subunit is directly connected to the Rieske center of a neighboring α-subunit by hydrogen bonds through a single amino acid, Asp 205, and, the substrate analogue indole binds such that the N atom of the pyrrole ring interacts with the amide of Asp205 (3.4 Å). Although no hydrogen bond acceptor is present in substrates such as naphthalene, it nevertheless indicates that the helix upon which the conserved amino acid lies may sense structural changes associated with substrate binding. Conversely, changes at the Rieske cluster associated with a change in redox state may influence events occurring at the mononuclear iron transmitted through Asp 205.

The current results thus show, for the first time, that the redox state of the Rieske center modulates the separation of the substrate and the catalytic non-heme iron of NDO. It is possible that the shift to the distal (B) site upon cluster reduction is required for O_2 to gain access to the iron, accounting for the observed lack of O_2 interaction with the enzyme when the Rieske center is oxidized. Note, however, that, during catalysis, the Rieske cluster becomes reoxidized as it transfers an electron to the oxygen-bound mononuclear center. Thus, the substrate may shift to the proximal (A) position during conversion from the O_2−ferro−NDO^R−naphthalene to $[O_2$−ferro$]^-$−NDO−naphthalene state that is critical to catalysis. Consequently, the shift in naphthalene position disclosed here may hold the key to both oxygen gating and oxygen reactivity by Rieske aromatic dioxygenases.

The spectra of the complexes with benzene and toluene $T = 20$ μs are not sufficiently well resolved to determine whether these substrates also exhibit A and B binding geometries, although the presence of a second deuteron signal in the $T = 60$ μs spectrum of NO−ferro−NDO^R−toluene suggests that this may be so, and that this substrate also experiences the allosteric linkage.

The NDO^R−indole structure led to the reasonable suggestion that alternate single-ring aromatic compounds may bind in the position of the naphthalene ring that is located farthest away from the Fe atom, to account for fact that, for the most part, these substrates are not oxidized in the same way as naphthalene. This hypothesis is not supported by the present study, although it remains possible that these alternative substrates also bind in another site too far from the iron to be detected. If this is the case, the site must be different than the B-site we have detected here, which is only slightly more displaced from the iron than the primary A-site binding location. Also, the spectra show that there is no net shift from the two nearby binding orientations

to a hypothetical distant site. These results suggest that observed products from the alternative substrates may result from comparatively rapid reactions that occur as the substrates sample low-occupancy binding orientations. This is plausible because the alternate substrates have smaller volumes and, thus, would not "fill" the naphthalene binding pocket. Apparently, the binding of the natural substrate naphthalene is sufficiently constrained to limit the alternative geometries that can be occupied.

Conclusions

The high-resolution electron nuclear double resonance (EN-DOR) data presented here provide the first detailed analysis of substrate binding to naphthalene 1,2-dioxygenase (NDO) containing an oxidized Rieske cluster, and these analyses are the first to study the structure of the mononuclear iron environment when an O_2-mimic is bound to mononuclear iron. Several new aspects of the NDO interaction with substrate have emerged from this study. *First*, NO binds with at least one solvent, which indicates that two exchangeable, probably adjacent, ligand positions are available on the mononuclear iron in NDO. This would permit consideration of either end-on or side-on oxygen binding. *Second*, substrates that preferentially undergo dioxygenase, monooxygenase, and uncoupling reactions during turnover all bind to NDO with similar geometries, despite the fact that different geometries would be expected, on the basis of the products observed. *Third*, the data lead to a precise model for the binding geometry of the natural substrate, naphthalene. Its agreement with a recent X-ray report[13] confirms that NO is a good surrogate for O_2 in this system, while showing that complexes formed *in low-temperature crystals* correspond to those in enzymes frozen after making complexes *in solution. Fourth,* reduction of the Rieske cluster, which creates the form of NDO that is reactive in single-turnover processes, causes an allosteric change in the active site, thus demonstrating that the redox state of the cluster and the substrate binding pocket are coupled. This observation provides evidence for a dynamic change in structure and reactivity within NDO during catalysis and may yield insight to the basis for the observation that substrate binding and Rieske cluster reduction gate the reaction with O_2 during the catalytic cycle.

Supporting Information Available: Q-band ENDOR spectra of NO−ferro−NDO complexes with substrates naphthalene, benzene, and toluene (PDF). This material is available free of charge via the Internet at http://pubs.acs.org.

JA0214126